Spatiotemporal profiles of somatosensory and insular cortical responses to mechanical stimulation of the periodontal ligament during experimental tooth movement

Mari Kaneko
Nihon University Graduate School of Dentistry
Major in Orthodontics
(Directors: Profs. Mitsuru Motoyoshi and Masayuki Kobayashi)

Index

This thesis is based on the following articles,

1) Physiological profiles of cortical responses to mechanical stimulation of the tooth in the rat: An optical imaging study.
   Mari Kaneko, Eri Horinuki, Noriyoshi Shimizu, Masayuki Kobayashi.
   Neuroscience. 358, 170-180, 2017.
2) Experimental tooth movement temporally changes neural excitation and topographical map in rat somatosensory cortex.
   Mari Kaneko, Satoshi Fujita, Noriyoshi Shimizu, Mitsuru Motoyoshi, Masayuki Kobayashi.
   Brain Research. 1698, 62-69, 2018.

Aim and Scope

The periodontal ligament (PDL) includes several types of nerve endings, such as Aβ-, Aδ-, and C-fibers, which play critical roles in detecting the strength and direction of occlusal force. Previous studies have demonstrated that electrical stimulation of the PDL activates the somatosensory and insular cortices. However, the profile of cortical excitation in response to mechanical PDL stimulation mostly remains unknown.

To investigate the differences in cortical responses to electrical and mechanical stimulation of the maxillary first molar, I performed optical imaging to determine the responding cortical regions in combination with a pharmacological approach. The molar was mechanically stimulated by pulling in the rostral direction, and electrical stimulation was applied via bipolar electrodes inserted into the mesial PDL. Mechanical stimulation initially excited the primary somatosensory cortex (S1), whereas electrical stimulation evoked an initial response between the secondary somatosensory cortex (S2) and insular oral region (IOR). The characteristic feature responding to mechanical stimulation was the rebound response evoked at the end of mechanical stimulation. A longer mechanical stimulation evoked a larger amplitude of the rebound response. A paired-pulse protocol of mechanical stimulation revealed that the amplitude of the second response was smaller than the first response, in accordance with the shorter interstimulus interval. Systemic application of morphine, a potent blocker of nociception, reduced the amplitude of the maximum excitation, particularly in S2/IOR compared to S1. These results suggest that S1 and S2/IOR are principally excited by mechanical and electrical stimulation, respectively, and that S2/IOR is involved in nociception processing.

During orthodontic treatment, binding teeth may change the topographically organized representation of teeth in the cerebral cortex. Thus, next, to test the hypothesis that experimental tooth movement (ETM) changes the somatotopy of an individual tooth arrangement in the somatosensory cortex, I examined the spatiotemporal features of cortical excitatory propagation in response to mechanical stimulation of the maxillary incisor or molar using optical imaging in late adolescent rats without or with ETM. The ETM models consisted of 1d, 3d, and 7d ETM in which a closed-coil spring was ligated between the maxillary first molar and incisors. In controls, incisor and molar mechanical stimulation evoked excitation in the rostral and dorsocaudal regions of S1, respectively. In addition, S2/IOR was also activated. Incisor stimulation-induced excitatory regions in S1 of 3d and 7d ETM shifted without changing the maximum excitatory area or peak amplitude; the incisor stimulation-responding region moved toward the dorsocaudal region, which responded to molar stimulation in the control. This shift in excitatory region was not observed in 1d ETM. One day after removal of the coil spring that was attached for 6 days, the excitatory region shift in S1 was recovered to the control region. On the other hand, 1d ETM exhibited facilitation of the excitatory area and peak amplitude upon molar stimulation, and the facilitation of excitatory propagation disappeared in 3d and 7d ETM.

These results may explain the clinical finding that abnormal sensation temporally occurs during orthodontic treatment.

Abbreviations

6d ETMR: 6 days ETM and 1 day after coil removal
CCD: charge-coupled device
ΔF: changes in the intensity of fluorescence
EMG: electromyography
ETM: experimental tooth movement
F: initial intensity of fluorescence
IC: insular cortex
IOR: insular oral region
ISI: interstimulus interval
MCA: middle cerebral artery
PDL: periodontal ligament
RF: rhinal fissure
S1: primary somatosensory cortex
S2: secondary somatosensory cortex

Chapter 1

Physiological profiles of cortical responses to mechanical stimulation of the tooth in the rat: An optical imaging study

Introduction

The PDL contains mechanoreceptors, including Ruffini endings (Byers, 1985) and Merkel cells (Tadokoro et al., 2002). These PDL receptors contribute to regulation of occlusal force and direction in harmony with muscle spindles in the jaw-closing muscles (Zhang et al., 2003; Lund and Kolta, 2006). The peripheral afferents innervating the PDL are classified as fast (rapidly) adapting, slowly adapting, and spontaneously firing subtypes (Ness, 1954; Hannam, 1969; Ishii et al., 2002). The rapidly adapting afferents exhibit short bursts of firing, whereas the slowly adapting afferents fire throughout the stimulation. The spontaneously firing subtype exhibits firing at rest and fires in a manner similar to the slowly adapting fibers responding to stimulation.

In a previous study, the populations of the rapidly and slowly adapting afferents were examined with an *in vitro* jaw-nerve preparation of the rat, and the results demonstrated that 61.5% and 38.5% of the afferents are rapidly and slowly adapting, respectively (Ishii et al., 2002). The rapidly adapting afferents are further divided into the ON type (64%), OFF type (2%), and ON-OFF type (35%): ON type afferents only fire at the beginning of stimulation; OFF type afferents only fire at the end of stimulation; and ON–OFF type afferents fire at both at the beginning and end of stimulation. These profiles of the primary afferents in the PDL suggest complex neuronal responses in the corresponding higher brain region including the cerebral cortex.

The cortical responses induced by mechanical stimulation of the PDL have been reported in the cat (Lund and Sessle, 1974; Watanabe et al., 1991; Nishiura et al., 2000) and in the monkey (Ogawa et al., 1989; Lin et al., 1994; Toda and Taoka, 2001). These studies have focused on the neural profiles such as the latency, firing probability, and receptive field, principally in S1. A noninvasive human brain imaging study revealed that the mechanical stimulation of the PDL induced activation in S1 and S2 (Habre-Hallage et al., 2014) or the insular and supplementary motor cortices (Ettlin et al., 2004), suggesting that several cortical regions in addition to S1 are also involved in mechanosensory information processing. However, little is known about the neural activity profiles responding to mechanical stimulation of the PDL in the cortical regions other than S1.

Nociceptive information of the dental pulp is integrated in rat S1, S2 and IOR (Shigenaga et al., 1974; Nakamura et al., 2015, 2016). In addition, similar cortical regions respond to

electrical stimulation of the PDL in the rat (Horinuki et al., 2015, 2016, Kobayashi and Horinuki, 2017), which suggests that S1 and S2/IOR are likely to integrate orofacial somatosensory information. Recently, my colleagues have demonstrated that sensation induced by stimulation of muscle spindles in the masseter (jaw closing) muscle, which respond to the stretching of the muscle (Kato et al., 1982), is processed both in S1 and S2/IOR (Fujita et al., 2017). Sensory information from muscle spindles and the PDL are considered to be coordinately organized to regulate orofacial movements, including mastication and occlusion (Morimoto et al., 1989), and therefore it is critical to elucidate the profile of cortical excitation that responds to mechanical stimulation of the PDL.

In the present study, optical imaging was performed to identify the cortical regions that respond to mechanical stimulation of the maxillary first molar and investigated the differences in cortical responses to electrical stimulation of the PDL and mechanical stimulation of the molar. In addition, morphine, the most potent blocker of nociception, was systemically applied to examine which cortical region was sensitive to nociception.

Materials and Methods

Forty-five male Sprague-Dawley rats (208.9 ± 6.9 g; 6-8-weeks-old; Japan SLC, Hamamatsu, Japan) were used in this study. The experimental protocol used in this study was approved by the Animal Experimentation Committee at Nihon University (AP15D047). The animal treatments were performed in accordance with the institutional guidelines for the care and use of experimental animals described in the National Institutes of Health's Guide for the Care and Use of Laboratory Animals.

Animals

The optical imaging technique was previously described (Fujita et al., 2012; Horinuki et al., 2015; Nakamura et al., 2015; Horinuki et al., 2016; Nakamura et al., 2016; Fujita et al., 2017), and a brief description of the procedure was provided below.

Atropine methyl bromide (5 mg/kg) was intraperitoneally injected, and the animals were anesthetized with urethane (1.4 g/kg, i.p.). Body temperature was monitored by a rectal probe and maintained at 37°C using a heating pad (BWT-100, Bio Research Center, Osaka, Japan). Lidocaine (2% gel, AstraZeneca, Tokyo, Japan) was used for complete analgesia. After removing the left temporal muscle and zygomatic arch (contralateral to stimulation), the IC and the surrounding cortices were exposed by a craniotomy. The urethane-anesthetized animal was fixed to a stereotaxic snout frame (Narishige, Tokyo, Japan) that was tilted 60° laterally to visualize S1 and S2/IOR by a charge-coupled device (CCD) camera (MiCAM02, Brainvision, Tokyo, Japan; Fig. 1A).

Optical Imaging

After fixation of the animals, the voltage-sensitive dye RH1691 (1 mg/ml, Optical Imaging, New York, NY, USA), which correlates with subthreshold membrane potential changes, was applied to the left cortical surface (contralateral to stimulation) for approximately 1 h. Fluorescent changes in RH1691 were measured by the CCD camera system mounted on a stereomicroscope (Leica Microsystems, Wetzler, Germany). A tungsten-halogen lamp (CLS150XD, Leica Microsystems) illuminated the cortical surface through a 632-nm excitation filter and a dichroic mirror. The fluorescent emission was captured through an absorption filter (λ > 650-nm longpass, Andover, Salem, MA, USA). The CCD camera had an imaging area (6.4 × 4.8 mm^2; 184 × 124 pixels).

To remove signals caused by acute bleaching of the dye, values without stimuli were subtracted from each recording. The sampling interval was set at 4 ms. Twenty-four consecutive images in response to the stimuli were averaged to improve the signal-to-noise ratio.

Mechanical and electrical stimulation

For mechanical stimulation, preformed ligature wires (diameter = 250 μm, Tomy International, Tokyo, Japan) were ligated to the right maxillary first molars (Fig. 1B). To ensure the ligation, the wires were fixed to the crown with dental cement (Estelite Flow Quick, Tokuyama Dental, Tokyo, Japan). The cranium was tightly fixed to the frame by dental cement (Super Bond, Sun Medical, Tokyo, Japan or Panavia V5, Kuraray, Tokyo, Japan) and Unifast Ⅲ (GC, Tokyo, Japan) to lessen the movement of the imaging area by the mechanical stimulation. Voltage pulses were applied to a motor unit (76011, Tamiya, Tokyo, Japan) using stimulators (SEN-3301, Electronic Stimulator, Nihon Kohden, Tokyo, Japan, and STG2008, Multi Channel Systems, Reutlingen, Germany) at 0.05 Hz to generate mechanical stimulation to the molar (Fig. 1A). The durations of the pulses were 100, 300, 500, and 1000 ms, and the intensity ranged from 0.11 to 0.29 N.

As the mechanical molar stimulation directly activates mechanoreceptors in the PDL, the principal organ mechanically stimulated is the PDL. However, I cannot exclude the possibility that mechanoreceptors not only in the PDL but also in the gingiva and alveolar bone are stimulated. Therefore, the stimulation induced by pulling the molar as the mechanical stimulation of the molar was described in this manuscript.

In addition, bipolar enamel-coated copper wire electrodes (diameter = 100 μm; Tamagawadensen, Tokyo, Japan) were inserted into the mesial PDL of the right maxillary first molar (Fig. 1B), and electrical stimulation was applied by five trains of voltage pulses (100 μs, 50 Hz, 5 V) at 0.05 Hz using the stimulator (STG2008, Multi Channel Systems). A static hydraulic testing system (5567 Dual Column Testing System, Instron Industrial Products, Gove City, PA, USA) was used to evaluate the tractive force induced by the motor unit during application of a voltage pulse (0.5-5.0 V, 100 ms), and data were analyzed using Bluehill2 (ver. 2.17, Instron Industrial Products). I confirmed the linear relationship between

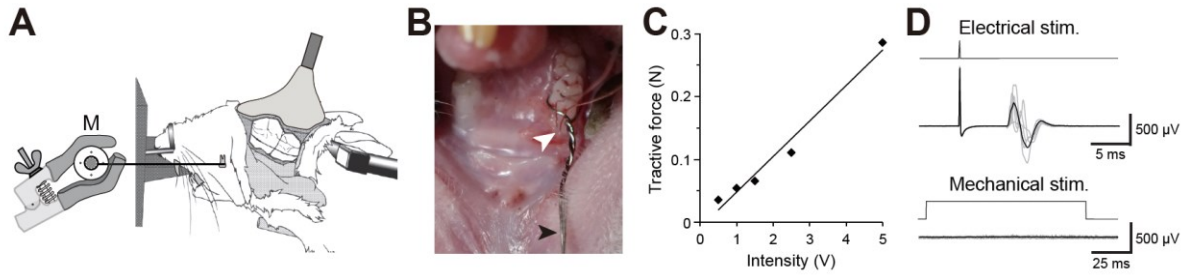

Figure 1. Experimental procedures. (A) A schematic drawing of the preparation for optical imaging of the somatosensory and insular cortices. To apply the mechanical stimulation to the maxillary first molar, a ligature wire ligated to the maxillary first molar was pulled by a motor unit (M). (B) For mechanical stimulation, a ligature wire was ligated to the cervical area of the right maxillary first molar (closed arrowhead). In addition, wire stimulation electrodes for electrical stimulation were inserted into the mesial PDL of the maxillary first molar (white arrowhead). This photograph was taken without bonding with dental cement to show the methods of stimulation clearly. (C) A scatterplot with a regression line demonstrating the linear relationship between the voltage intensity applied to the motor unit and tractive force ($R^2 = 0.98$). (D) The EMGs responding to the electrical (5 V) or mechanical (~0.29 N) stimulation to the maxillary first molar. The averaged traces (black) are superimposed on 5 raw traces (gray).

the voltage intensity applied to the motor unit and the tractive force ($R^2 = 0.98$; Fig. 1C).

Electromyography

To examine whether mechanical stimulation of the molar and electrical stimulation of the PDL induce nociception, the electromyography (EMG) was recorded from a jaw-opening muscle. Bipolar enamel-coated copper wire electrodes (diameter = 100 μm; Tamagawadensen) were inserted into the right anterior part of the digastric muscle (ipsilateral to stimulation). The EMG activity responding to mechanical or electrical stimulation was recorded using an amplifier (Nihon Kohden, Tokyo, Japan), A-D converter (CED1401, Cambridge Electronic Design, Cambridge, U.K.), and data acquisition system (Spike 2, Cambridge Electronic Design). Sampling rate was set at 10 kHz.

Drugs

To obtain analgesic condition, morphine (Daiichi-Sankyo, Tokyo, Japan) dissolved in saline was injected subcutaneously into the backs of the rats. The dose of morphine was set at 2.5 mg/kg with reference to the previous study (Guo et al., 2010). Optical signals were recorded 15-25 min after injection. As a vehicle control, saline (0.5 ml/kg) was injected subcutaneously into the backs.

Histology

After optical imaging, the animals were perfused with 4% paraformaldehyde in 0.1 M phosphate buffer (PB), and the brains were removed and stored in fixative overnight at 4°C. Then, the brains were immersed into 30% sucrose in 0.1 M PB for 3-4 days until they sank. Sections were cut with a freezing microtome (SM2000R, Leica) at 50-μm thickness. Coronal

sections were immersed in a solution containing 0.05% cytochrome C obtained from equine heart (C2506, Sigma-Aldrich, St. Louis, USA), 0.08% 3,3'-Diaminobenzidine (D0078, Tokyo Chemical Industry, Tokyo, Japan), 4% sucrose, and 0.1 M PB, and then incubated at 37°C for 2–6 h in the dark until layer IV in S1 was visible (Wong-Riley, 1979). After three rinses for 7 min in 0.1 M PB, sections were mounted on gelatin-coated slides, air-dried, dehydrated in ethanol, cleared in xylene, and cover-slipped. Stained sections were imaged using a microscope (BZ-9000, Keyence, Osaka, Japan). Minor adjustments of image brightness and contrast were performed in Adobe Photoshop (ver. CC 2014; Adobe Systems, San Jose, USA). The final schematic figures were generated using Adobe Illustrator (ver. CC 2014; Adobe Systems).

Data Analysis

Changes in the intensity of fluorescence (ΔF) in each pixel were divided by the initial intensity of fluorescence (F), and the ratio (ΔF/F) was processed with a spatial filter (9 × 9 pixels). A significant response was defined as a signal that exceeded 7 times that of the standard deviation of the baseline noise. The optical imaging data were processed and analyzed using Brain Vision Analyzer (Brainvision).

To quantitatively analyze the spatiotemporal profiles of excitation, I used the initial and maximum excitation areas and the peak amplitude at the center of the initial response. The initial response was obtained by outlining the evoked excitation in the first frame that exhibited a significant increase in the optical signal. The maximum response was defined as the frame with the maximum amplitude of the optical signal in the center of excitation (Fig. 2).

The EMG activity was quantified by measuring the peak amplitude of the responses to the mechanical or electrical stimulation from the baseline.

Data are expressed as the means ± standard error of the mean (SEM). Paired *t*-test was used to compare the latency, peak amplitude, half width, 20-80% rise time, and 80-20% decay time of responses between S1 and S2/IOR. The effects of morphine on the optical signals and digastric EMG was also statistically analyzed by paired *t*-test. $P < 0.05$ was considered significant. Student's *t*-test with Bonferroni correction was used for intensity-dependent signal changes, rebound ratio, and paired-pulse ratio. In this test, the significance level was set at $P < 0.016$.

Results

In vivo optical imaging was performed to measure the optical signals in the somatosensory and insular cortices responding to electrical of the PDL or mechanical stimulation of the molar. The differences in the response profiles between electrical and mechanical stimulation was clarified. Furthermore, opioidergic effects on the cortical excitation were examined to explore how nociceptive inputs contribute to excitatory propagation in S1 and S2/IOR.

EMG activities to electrical and mechanical stimulation of the molar

Jaw-opening reflex is a good indicator to detect noxious inputs in the oral region (Mason et al., 1985), and therefore, I recorded the EMG activities from the anterior part of the digastric muscle to define the threshold of jaw-opening reflex (Fig. 1D). Electrical stimulation of the PDL (5 V) induced the consistent EMG activities in the digastric muscle: 452.0 ± 137.5 μV (n = 6). In contrast, mechanical stimulation (5 V) to the molar induced the ignorable EMG activities (25.4 ± 4.4 μV, n = 5). These results suggest that nociception is induced by electrical but not mechanical stimulation.

The initial responses to electrical and mechanical stimulation

Fig. 2 shows a typical example of cortical responses to electrical stimulation of the PDL and mechanical stimulation of the molar. Similar to my colleagues' previous reports (Horinuki et al., 2015, 2016), electrical stimulation of the molar PDL (5 V) initially activated the caudal region adjacent to the middle cerebral artery (MCA; Fig. 2A,B, white circle), and then the region rostral to the MCA was activated (Fig. 2A,B, black circle). On the other hand, mechanical stimulation of the molar initially activated the region rostral to the MCA (Fig. 2D,E, black circle), and then the region caudal to the MCA was activated (Fig. 2D,E, white circle).

To examine the cytoarchitecture of these activated regions, I performed cytochrome staining using coronal sections with lesions that were located in the center of the rostral and caudal regions activated by electrical and mechanical stimulation of the first molar (Fig. 2G). The lesion corresponding to the initial response of the mechanical stimulation of the maxillary first molar was located in the rostral S1 (Fig. 2Gb), which is characterized by dense staining in layer IV. Similarly, the initial response to electrical stimulation of the maxillary first molar was located in the rostral portion of S1 (Fig. 2Ga), which is located on the opposite side of S2/IOR in reference to the MCA (Fig. 2Gc).

The latency of S1 excitation induced by electrical stimulation of the maxillary first molar PDL was 16.7 ± 0.6 ms (n = 12; Fig. 2C), which was longer than that of S2/IOR (11.0 ± 0.5 ms, n = 12; $P < 0.001$, paired *t*-test). In contrast, mechanical stimulation of the maxillary first molar evoked the initial response in the region rostral to the MCA, i.e., S1, and then S2/IOR was activated. The latency in S1 (22.2 ± 2.2 ms, n = 13) was shorter than that in S2/IOR (28.9 ± 2.5 ms, n = 13; $P < 0.05$, paired *t*-test). Comparison of the latencies between the electrical and mechanical stimulation was not performed (see Discussion).

Spatial distribution profiles of evoked responses to mechanical stimulation

The initial and maximum responses were superimposed with reference to the MCA and rhinal fissure to identify the somatotopic distribution pattern of cortical responses to electrical (n = 7) and mechanical stimulation of the maxillary first molar (n = 9-12; Fig. 3). As described in the typical example (Fig. 2), electrical stimulation of the maxillary first molar PDL induced excitation in the region caudally adjacent to the MCA (Fig. 3A), whereas the initial responses

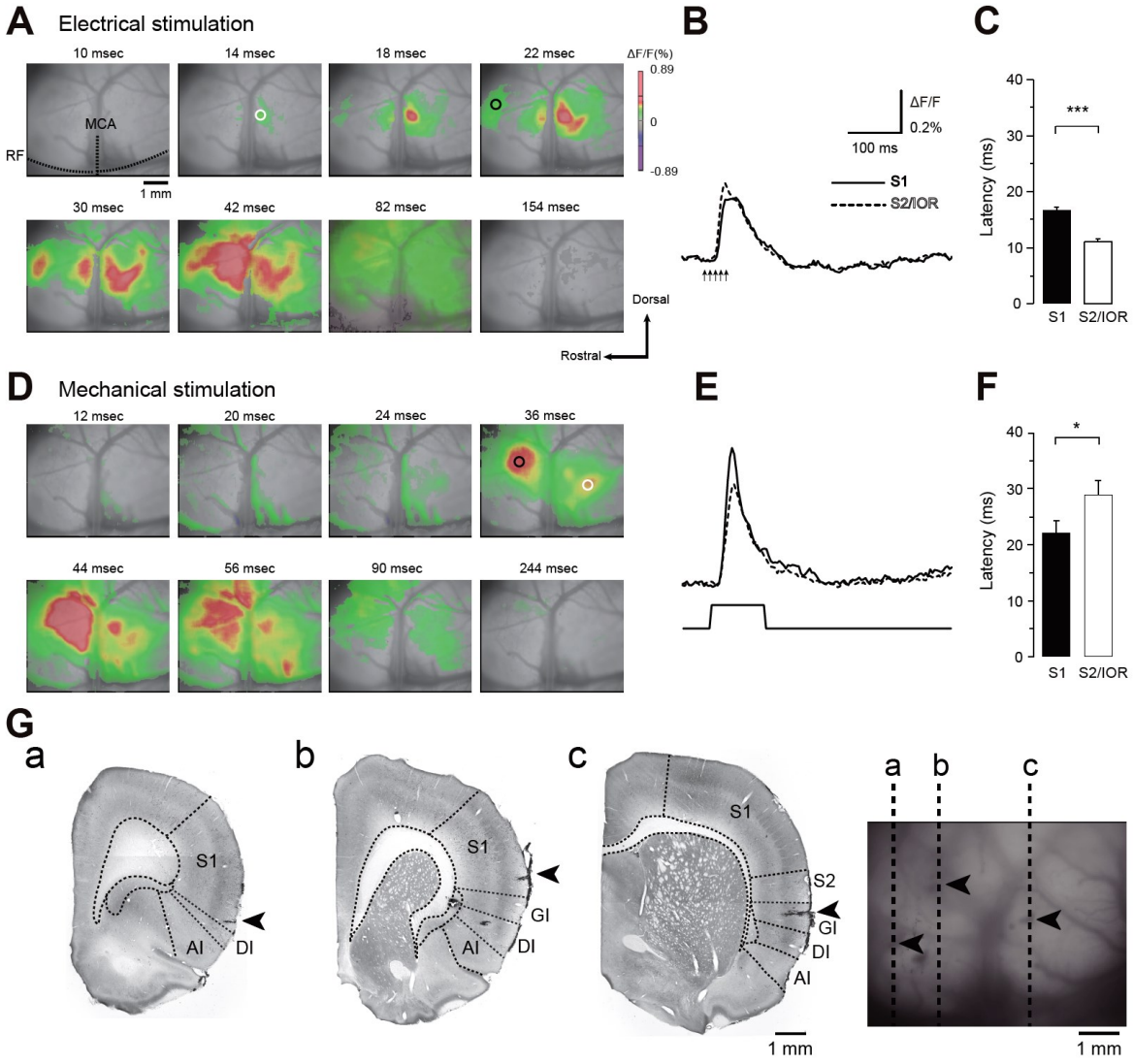

Figure 2. Spatiotemporal profiles of the initial responses to electrical and mechanical stimulation of the maxillary first molar. (A) Optical signals evoked by electrical stimulation (5 pulses at 50 Hz, 5 V). The ratio of ΔF/F was color coded, and the time from the stimulation onset is shown at the top of each panel. The white and black circles indicate the center of initial response in S2/IOR and S1, respectively. (B) Temporal profiles of optical signals induced by electrical stimulation at the center of excitation marked with black (S1) and white (S2/IOR) circles in (A). Arrows indicate the timing of electrical stimulation. (C) Comparison of the latency of cortical responses to electrical stimulation in S1 (black) and S2/IOR (white). (D) Color-coded signals evoked by mechanical stimulation (duration: 100 ms, 5 V). (E) Temporal profiles of optical signals induced by mechanical stimulation. The square wave pulse indicates the voltage applied to the motor unit. (F) Comparison of the latency between the S1 and S2/IOR responses to mechanical stimulation. (G) Cytochrome oxidase-stained sections with lesions (closed arrowheads). The lesion at the center of initial response evoked by electrical stimulation (c) was located in S2/IOR. The initial response to mechanical stimulation (b) was observed in S1. The rostral region activated by electrical stimulation (a) was located in S1. *$P < 0.05$. ***$P < 0.001$. RF, rhinal fissure; MCA, middle cerebral artery; S1, primary somatosensory cortex; S2, secondary somatosensory cortex; AI, agranular insular cortex; DI, dysgranular insular cortex; GI, granular insular cortex.

to mechanical stimulation were principally located in S1, which was rostral to the activated region in S2/IOR (Fig. 3B).

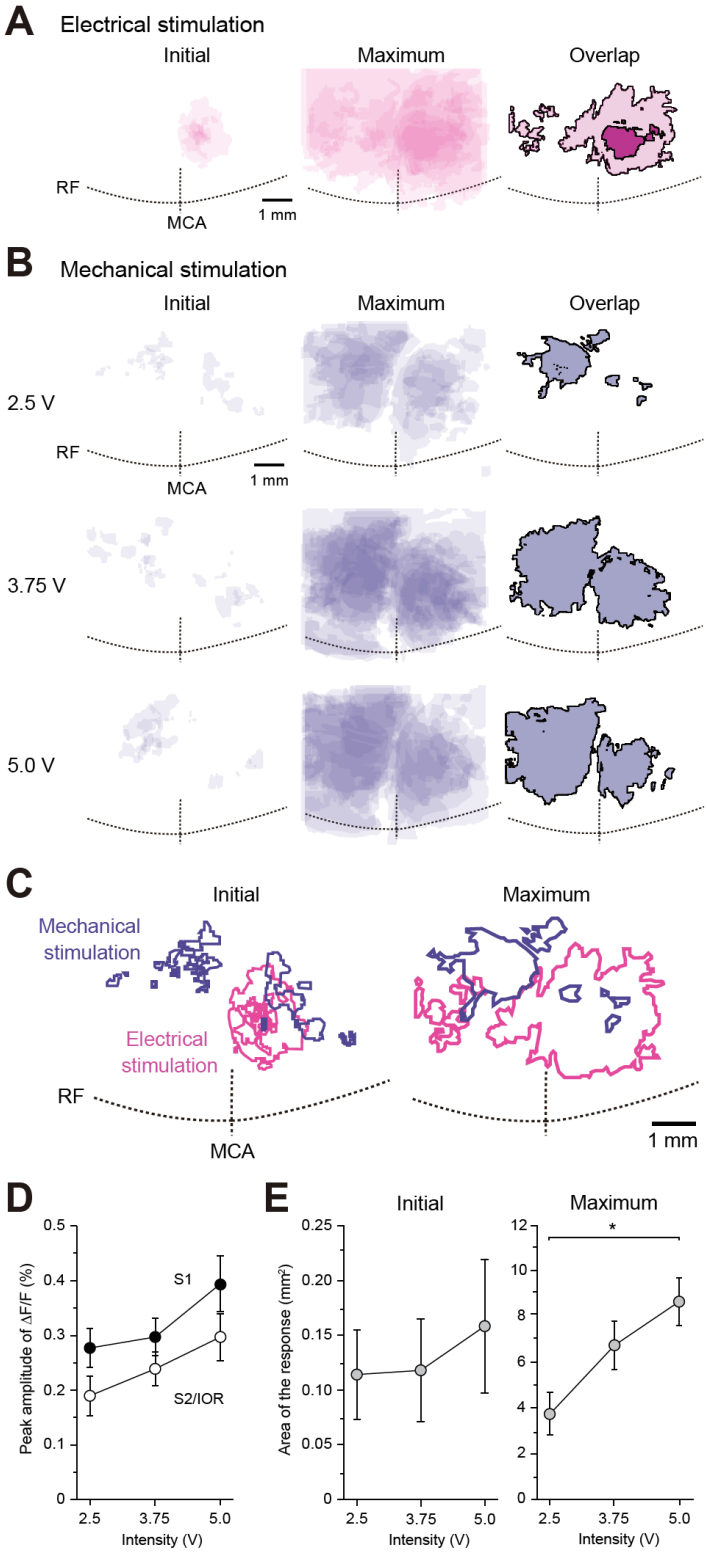

Figure 3. Spatial patterns of the initial and maximum responses to electrical and mechanical stimulation. (A) The initial (left) and maximum responses (middle) to electrical stimulation (5 V) were superimposed with reference to the MCA and RF (n = 7). The two-tone colored map (right) indicates the overlapping area of the maximum responses in 50% of the rats (light color) and 100% of the rats (deep color). (B) The initial and maximum responses and two-tone colored maps responding to mechanical stimulation (2.5 V; n = 9, 3.75 V; n = 12, 5.0 V; n = 12). (C) Superimposed outlines of the initial and maximum responses induced by electrical (A) and mechanical stimulation (B; 2.5 V) are shown on the left and right columns, respectively. (D) Peak amplitudes evoked by mechanical stimulation are plotted against the stimulation intensity. (E) The intensity-dependent changes in the responding area to the mechanical stimulation. *$P < 0.05$.

The maximum responses to the electrical and mechanical stimulation of the first molar were observed both in S1 and S2/IOR (Fig. 3A,B). Excitation was initially induced in the restricted region of S1 and S2/IOR and propagated in a concentric manner. The increase in the excitatory propagation induced by mechanical stimulation was dependent upon the voltage intensity driving the motor unit (Fig. 3B,D,E).

Fig. 3C shows the superimposed outlines of the cortical responses to electrical and mechanical stimulation of the maxillary first molar. The initial excitatory region that appeared in response to mechanical stimulation of the maxillary first molar differed from that induced by electrical stimulation. In S1, the maximum responses to electrical stimulation were observed in the ventrorostral portion (Fig. 3A,C), whereas mechanical stimulation activated the dorsocaudal portion (Fig. 3B,C). These findings demonstrate that the cortical responses to electrical and mechanical stimulation of the maxillary first molar were spatially segregated in S1 but almost overlapped in S2/IOR.

Rebound responses to mechanical stimulation

It has been reported that the rapidly adapting neurons that respond to mechanical stimulation of the PDL are divided into ON-type, OFF-type, and ON-OFF type (Ishii et al., 2002). The sensory information is processed in the trigeminal sensory nucleus and the thalamic ventral posteromedial nucleus and is then projected to the somatosensory cortex (Linden, 1990). Periodontal mechanosensitive neurons in S1 are classified as slowly adapting, rapidly adapting, and spontaneously discharging (Ness, 1954; Taira, 1987). To understand how these types of neurons were activated by mechanical stimulation of the molar in the cerebral cortex, I changed the duration of the mechanical stimulation to the maxillary first molar (duration; 100, 300, 500, 1000 ms) and analyzed the duration-dependent responses.

As expected, the cortical excitation evoked by mechanical stimulation occurred not only at the start of stimulation but also at the end of stimulation (Fig. 4). The response observed at the start of stimulation was defined as the first response, and the excitation in response to the end of stimulation was defined as the rebound response. The rebound ratio was calculated by dividing the peak amplitude of the rebound responses by the amplitude of the first response. At the 100-ms duration, the rebound responses were too small to detect. However, the rebound ratio where the stimulating duration was set at 300 ms was significantly increased in comparison to that at 100 ms (Fig. 4B,C; n = 8, $P < 0.016$, Student's *t*-test). The rebound responses in S1 and S2/IOR increased with the duration of the stimulation (Fig. 4C). The rebound signals were specific for mechanical stimulation and were considered to reflect the response properties of the first order neurons that innervate the PDL (Ishii et al., 2002).

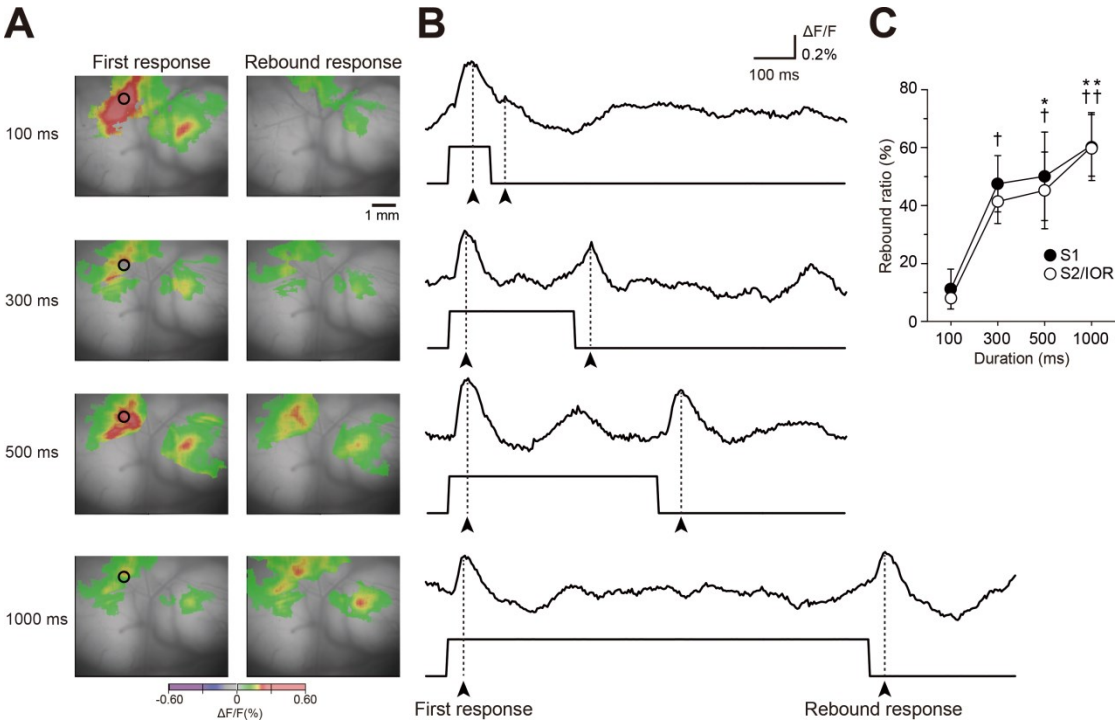

Figure 4. Rebound responses to mechanical stimulation of the molar. (A) The first (left) and rebound responses (right) are obtained at the timing shown in the left and right arrowheads in (B), respectively. The duration of mechanical stimulation was set at 100, 300, 500, and 1000 ms. (B) Temporal profiles of optical signals obtained from the center of the initial responses in S1 (black circles) shown in (A). (C) The rebound ratios are plotted against the duration of mechanical stimulation. The rebound responses in S1 and S2/IOR increased as the duration of stimulation became longer. Each rebound ratio is compared to that at 100-ms duration. *$P < 0.016$, **$P < 0.003$, in S1 (n = 8). †$P < 0.016$, †††$P < 0.0003$, in S2/IOR (n = 9).

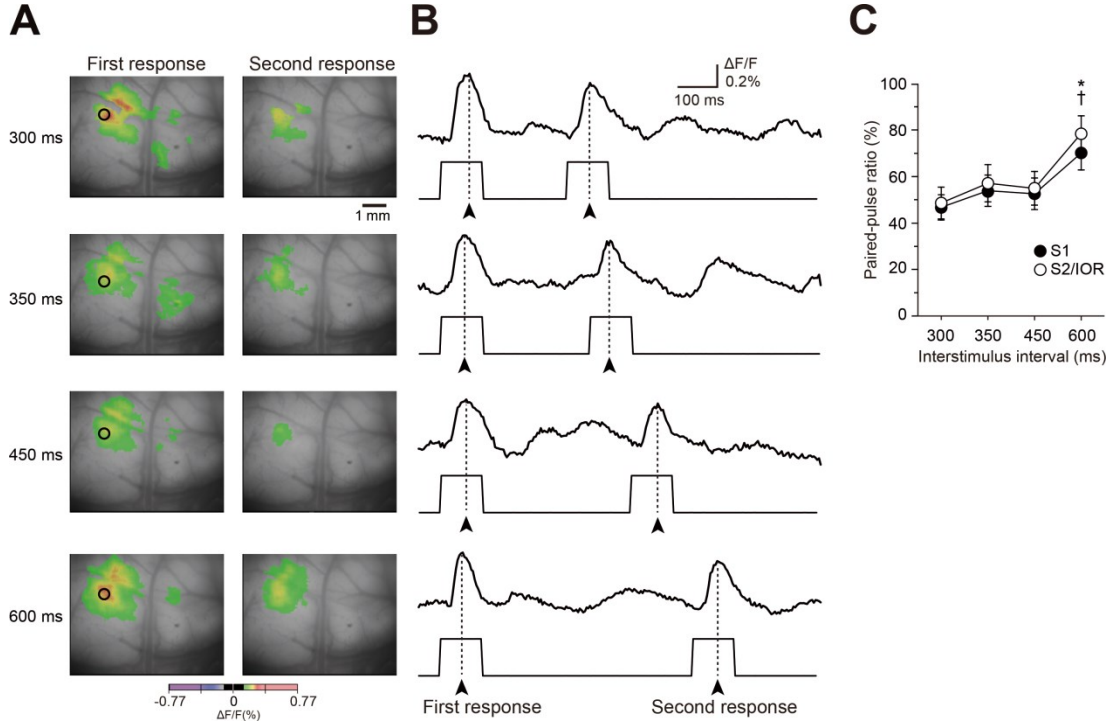

Figure 5. Short-term plasticity of the cortical responses to paired-pulse stimulation of the molar. (A) Typical examples of cortical responses to paired-pulse stimulation. The interstimulus interval (ISI) was set to 300, 350, 450, and 600 ms. (B) The temporal profiles of the optical signals at the center of excitation marked with black circles in (A). The peak amplitude of the second responses recovered as the ISI was prolonged. (C) Paired-pulse ratio is plotted against the ISI. Each paired-pulse ratio is compared to that at 300-ms ISI. *$P < 0.016$, in S1 (n = 14). †$P < 0.016$, in S2/IOR (n = 14).

Paired-pulse stimulation

I next examined how the temporal profiles of optical signals induced by mechanical stimulation change depending on the interstimulus interval (ISI). The paired-pulse stimulation to maxillary first molar was applied, and the ISI was set at 300, 350, 450, and 600 ms (Fig. 5). Paired-pulse depression was observed at all ISI, which gradually recovered as the ISI was prolonged. At the 600-ms ISI, the paired-pulse ratio significantly increased in comparison to those at the 300-ms ISI both in S1 and S2/IOR (Fig. 5C; n = 14; $P < 0.016$, Student's *t*-test).

Morphine depresses S2/IOR excitation

The difference in the spatiotemporal profiles of cortical excitatory propagation responding to electrical and mechanical stimuli may be due to differences in the stimulated fibers in the PDL. Electrical stimulation may activate both nociceptive and mechanoreceptors, while mechanical stimulation is likely to activate only mechanoreceptors. If this is the case, a region principally excited by electrical stimuli may exhibit a diminished response following application of morphine, a potent antinociceptive opiate (Kieffer and Gaveriaux-Ruff, 2002). To examine this possibility, I analyzed the effects of subcutaneous application of morphine (2.5 mg/kg), which suppressed the jaw-opening reflex by 55.9 ± 15.1% (n = 6; $P < 0.05$, paired *t*-test; Fig. 6F), on the excitatory propagation induced by electrical stimulation of the PDL.

Electrical stimulation of the maxillary first molar PDL induced cortical excitation even under subcutaneous application of 2.5 mg/kg morphine (Fig. 6). However, the excitatory propagation in S2/IOR was more potently depressed compared to that in S1 (Fig. 6A,B). To quantify this finding, the kinetics of the optical signal amplitude in the initially activated sites in S1 and S2/IOR was compared between the control and the morphine application (Fig. 6C). Morphine significantly decreased the maximum amplitude of optical signals from 0.30 ± 0.03 to 0.22 ± 0.03 (29% depression; n = 9, $P < 0.001$; paired *t*-test) in S2/IOR, whereas morphine had little effect on the maximum amplitude in S1 (Fig. 6Ca; n = 9, $P > 0.127$; paired *t*-test). Interestingly, the decay kinetics of the signals showed a significant increase: 80-20% decay time was increased from 66.3 ± 7.4 ms to 72.6 ± 10.4 ms in S2/IOR and 52.0 ± 3.2 ms to 91.4 ± 13.5 ms in S1 (n = 7; Fig. 6Cd; $P < 0.05$, paired *t*-test). The half duration was also prolonged from 34.7 ± 6.7 ms to 68.4 ± 8.8 ms in S2/IOR and 73.8 ± 6.7 ms to 95.6 ± 9.1 ms in S1 (n = 9; Fig. 6Cb; $P < 0.05$, paired *t*-test). Saline injection as a vehicle control induce no significant changes in the maximum amplitude either in S2/IOR (0.329 ± 0.047% to 0.323 ± 0.040%, n = 6; $P > 0.62$, paired *t*-test) and in S1 (0.239 ± 0.033% to 0.245 ± 0.035%, n = 6; $P > 0.57$, paired *t*-test).

In parallel to the decrease in the amplitude of excitation, the maximum area of excitation was decreased especially in S2/IOR (Fig. 6D,E; $P < 0.05$, paired *t*-test). These results support the hypothesis that S2/IOR is involved in nociception processing, whereas S1 mediates the mechanosensation.

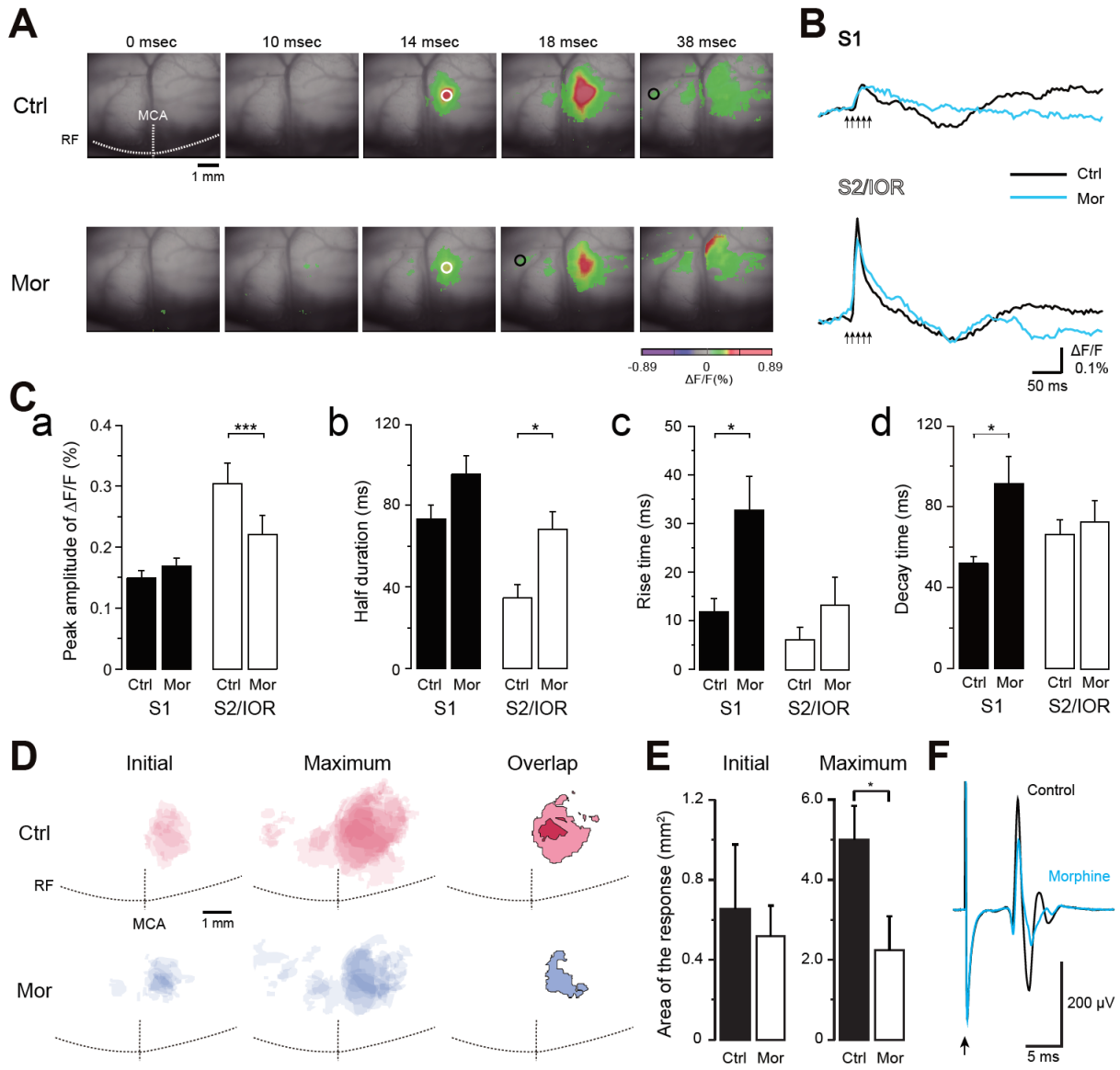

Figure 6. The effects of morphine on cortical excitatory propagation evoked by electrical stimulation of the PDL. (A) Color-coded signals induced by electrical stimulation in control (Ctrl, upper) and after application of morphine (Mor, lower). Excitation was first induced in S2/IOR, and then S1 was activated. (B) Optical signals obtained from S1 (black circles) and S2/IOR region (white circles) shown in (A) in control (black) and after morphine application (blue). (C) Peak amplitude (a), half duration (b), 20-80% rise time (c), and 80-20% decay time (d) observed in S1 (black) and S2/IOR (white) in control and after morphine application (n = 9). (D) The initial (left) and maximum (middle) responses in control (upper) and after morphine application (lower) are superimposed with reference to the MCA and RF (n = 9). Two-tone colored maps (right) indicate the overlapping areas in 50% of rats (light color) and 100% of the rats (deep color). (E) The effects of morphine on the initial (left) and maximum excitation (right) areas. (F) The digastric EMG in response to the electrical stimulation (arrow) was suppressed by morphine (blue). *$P < 0.05$. ***$P < 0.001$.

Discussion

In the previous animal studies, the cortical responses to mechanical stimulation of the PDL have principally focused on S1 (Ogawa et al., 1989; Watanabe et al., 1991; Lin et al., 1994; Nishiura et al., 2000; Toda and Taoka, 2001). However, fMRI studies in the human have

demonstrated other cortical areas such as S2, insular, and supplementary motor cortices are involved in the information processing of the PDL mechanosensation (Ettlin et al., 2004; Habre-Hallage et al., 2014). Although Lund and Sessle (1974) reported neural activities of the presylvian and anterior orbital gyri, the neural profiles of PDL-responding neurons in the cortical regions except for S1 have been poorly understood. This study confirmed the excitation of S1 and S2/IOR in response to electrical stimulation of the PDL as previously my colleagues have reported (Horinuki et al., 2015, 2016), and extended them by demonstrating that mechanical stimulation to the maxillary first molar induced excitation in both S1 and S2/IOR. I clarified the differences in the response kinetics between electrical and mechanical stimulation: (1) mechanical stimulation induced greater or at least equivalent excitation in S1 compared to that in S2/IOR, and (2) mechanical stimulation evoked excitation not only to the initial phase (ON response) but also to the terminal phase of stimulation (OFF response). Systemic application of morphine effectively diminished S2/IOR excitation by electrical stimulation of the PDL in comparison to S1. This finding suggested different roles for S1 and S2/IOR in somatosensory information processing in the PDL, though I cannot exclude the possibility that mechanoreceptors not only in the PDL but also those in the gingiva and alveolar bone are stimulated by mechanical stimulation of the molar.

Spatial differences in activated regions between electrical and mechanical stimulation

Both electrical and mechanical stimulation activated S1 and S2/IOR; however, the spatial patterns of cortical excitation were different: the regions initially activated by electrical and mechanical stimulation were in S2/IOR and S1, respectively. In the present study, the mechanical stimulation was set at 2.5-5 V, which induced the tractive force from ~0.1 N to ~0.3 N (Fig. 1C). In this range, the mechanical stimulation of the molar did not induce jaw-opening reflex, suggesting that the mechanical stimulation was not noxious. Electrical stimulation of the PDL is likely to activate most afferents, including Aβ, Aδ, and C fibers, whereas mechanical stimulation principally activates Aβ fibers, which have a faster conduction velocity than Aδ and C fibers. If this is the case, electrical stimulation involves few Aβ fibers, and therefore the population of Aβ fibers that are activated by mechanical stimuli is small. As a result, the summation of the excitatory postsynaptic potentials would be small, and the latency of spike induction might be prolonged. Therefore, activation of S2/IOR that was principally induced by activation of nociceptive fibers may show a shorter latency than that induced by a small population of Aβ fibers.

Because the latency of excitation induced by mechanical stimulation was not precise compared to that induced by electrical stimulation, I cannot estimate the accurate latency of cortical excitation via Aβ fibers. Therefore, the above mentioned hypothesis is difficult to examine by precise measurement of the latency of excitation induced by each fiber. Alternatively, I pursued this issue using the pharmacological approach as discussed in the following section.

S2/IOR is more sensitive to morphine than S1

Morphine is a representative opioid, which suppresses the trigeminal nociceptive pathway (Dallel et al., 1996; Tzabazis et al., 2005; Luccarini et al., 2006; Guo et al., 2010; Kuki et al., 2014). The protocol for application of morphine was determined with reference to the previous studies on the orofacial pain. The study using the orofacial formalin test demonstrates that subcutaneous injection of morphine dose-dependently inhibits the face-rubbing response and the ED50 for this inhibition is 2.45 mg/kg (Luccarini et al., 2006). Guo et al. (2010) show that subcutaneous application of 0.4 mg/kg morphine significantly suppresses mechanical sensitivity and the suppressive effect of morphine is peaked at 4.0 mg/kg. The concentration of morphine used in the present study, i.e. 2.5 mg/kg, is in the range of effective doses. Indeed, administration of 2.5 mg/kg morphine induced depression of the amplitude of evoked the EMG responding to the electrical stimulation of the PDL, i.e. the jaw-opening reflex (Fig. 6F), suggesting a partial inhibition of nociception by morphine. However, I have to pay attention to the possibility that even low dose of morphine application may attenuate not only nociception but also other sensory inputs mediated via Aβ fibers (Yeomans et al., 1995).

Morphine suppresses nociception by several mechanisms, including the inhibition of voltage-sensitive calcium channels (McDonald and Lambert, 2005, 2013), the activation of G-protein inwardly rectifying potassium channels, and the decrement of the hyperpolarization-activated current, Ih, by the reduction of cAMP (McDonald and Lambert, 2005; Zollner and Stein, 2007). These opioidergic effects are observed at various levels from the spinal cord to the cerebral cortex. For instance, local injection of morphine into the IC suppresses nociceptive information processing at the dorsal horn (Burkey et al., 1996). These findings support the idea that systemic injection of morphine suppresses nociception and as a result neuronal activities in the nociception-related cortical region are likely to be diminished by morphine.

The present study demonstrates that S2/IOR was more sensitive to morphine than S1, which suggests that S2/IOR but not S1 is involved in nociceptive information processing. Although the excitability of S1 and S2/IOR are modulated by opioidergic receptor agonists as my colleagues previously showed (Yokota et al., 2016a, b), they observed rather homogenous suppression of excitatory propagation in S1 and S2/IOR by a μ opioidergic receptor agonist. Therefore, I suspect that the region-specific suppression of excitation by morphine may be due to different pathways from the trigeminal nuclei to the cerebral cortex.

Sex differences have been reported in chronic craniofacial pain, e.g. trigeminal neuralgia, atypical odontalgia, and temporomandibular joint disorders (Woda and Pionchon, 2000; Bereiter and Okamoto, 2011). Only male rats were used in this study, and there is a possibility that the response may be different in female rats. This should be further explored in the future.

Temporal profiles of mechanosensation in S1

In comparison to the responses to PDL electrical stimulation, the characteristic feature of the

response to mechanical stimulus was the off-response that was observed at the offset of mechanical stimuli. This feature is considered to reflect the physiological profiles of the primary afferents (Ness, 1954; Hannam, 1969; Ishii et al., 2002), i.e., OFF and ON-OFF type afferents (Ishii et al., 2002). On the other hand, I rarely observed a persistent increase in optical signals responding to a long mechanical stimulation (Fig. 4). Although I cannot exclude the possibility that a subset of S1 or S2/IOR neurons are activated during the mechanical stimuli, most these neurons are likely to exhibit maximum firing at the onset and offset of the mechanical stimulation pulses. This feature may contribute to physiological properties during tooth contact, which shows easy adaptation.

After mechanical stimulation of the molar, optical signal oscillation was often observed as shown in Figs. 4 and 5. The frequency of this oscillation was approximately 5-10 Hz, and this may reflect a portion of cortical activity under anesthesia. Paired-pulse stimuli at a certain interval could enhance or diminish the oscillatory activities, and therefore it is worth noting how the mechanical peripheral inputs modulate membrane oscillation in S1 and S2/IOR. However, the optical signals in this study were obtained by averaging 24 trials and were not substantial enough to estimate their fine temporal kinetics.

Functional cooperation between PDL and muscle spindles

Both the PDL and muscle spindles in the jaw-closing muscles functionally cooperate to detect objects in the oral cavity and control occlusal force. Their capacity for detection is rigorously controlled, and as a result I can easily detect a hair between our maxillary and mandibular teeth. Despite the finely controlled and cooperative function of these structures, their cortical topography was unknown.

Recent studies have demonstrated that electrical or mechanical stimulation of the muscle spindle afferents induces activation in the region caudally adjacent to the molar pulpal region (Fujita et al., 2017), which is also activated by PDL stimulation (Horinuki et al., 2015, 2016). Furthermore, the rostral portion of S1 responds to mechanical stimulation of the muscle spindle afferents (Fujita et al., 2017). Altogether, the present findings indicate that somatosensory information from the PDL and muscle spindles in the jaw-closing muscles project to adjacent regions in the S2/IOR. Such topographical differences in S1 and S2/IOR suggest differential information processing of the PDL and muscle spindles, even though these sensations may finally be integrated in these cortical regions.

Chapter 2

Experimental tooth movement temporally changes neural excitation and topographical map in rat somatosensory cortex

Introduction

Orthodontic treatment uses brackets and wires to bind teeth in order to fix their spatial arrangement in the oral cavity. During this treatment, the teeth are moved in response to orthodontic force, which activates osteoclasts and osteoblasts (Jiang et al., 2015; Lee et al., 2015) and leads to inflammation of the PDL (Vandevska-Radunovic, 1999; Krishnan and Davidovitch, 2006). My colleagues have demonstrated that electrical stimulation of the PDL during experimental tooth movement (ETM) induces hyperexcitability of S2/IOR (Horinuki et al., 2015, 2016), both of which receive noxious inputs from the orofacial area (Nakamura et al., 2015, 2016). In addition, the hyperexcitability of S2/IOR correlates with the severity of the PDL inflammation (Horinuki et al., 2016). This observation likely reflects the nociceptive mechanisms that occur during orthodontic treatment (Kobayashi and Horinuki, 2017). Indeed, the hyperexcitation of S2/IOR peaks one day after treatment and recovers to the control level within a week; the temporal profile of this hyperexcitation is similar to that of pain observed during clinical orthodontic treatment (Ngan et al., 1989; Krishnan, 2007).

Presentation of simultaneous somatosensory stimuli to adjacent organs combines the somatosensory cortical regions responding to each receptive field. For instance, pairing whiskers changes the response profiles of neurons in the barrel cortex, a part of S1 where cortical regions responding to a part of the body are somatotopically organized (Sood et al., 2015). A barrel cortical neuron exhibits a selective response to principal whisker stimulation, and after paring with the adjacent whiskers, the neuron begins to respond not only to the principal whisker but also to the paired whisker (Diamond et al., 1993). During ETM, the bound teeth receive simultaneous mechanical stress. Therefore, in addition to the hypernociceptive response in S2/IOR, ETM may induce another type of plastic change in S1.

To test the hypothesis that ETM changes the somatotopy of an individual tooth arrangement in the somatosensory cortex, cortical responses to mechanical stimulation were recorded by an optical imaging technique using ETM models whose maxillary incisors and right molar were bound with a coil spring (Fig. 1). ETM-induced changes were found in the somatotopic organization of S1 that continued for at least a week and recovered within a day after removal of a coil spring.

Materials and Methods

The experimental procedure was approved by the Animal Experimentation Committee at Nihon University (AP15D047). The animal treatments were performed in accordance with the institutional guidelines for the care and use of experimental animals described in the National Institutes of Health Guide for the Care and Use of Laboratory Animals. The materials and methods in this study were similar to those of my colleagues' and my previous studies (Horinuki et al., 2016; Kaneko et al., 2017), and therefore, I described them briefly.

Animals and ETM

Male Sprague-Dawley rats (6-7 weeks old; 205.4 ± 5.1 g, n = 63) received a treatment in which stainless wires (250 μm diameter, Tomy International, Tokyo, Japan) were fixed to the maxillary incisors and right molar (Fig. 1A). ETM was performed by binding the incisors and molar with a nickel-titanium coil spring (50 gf, Tomy, Tokyo, Japan; Fig. 1A). Four types of ETM models were made as follows: 1 (1d ETM), 3 (3d ETM), 7 days (7d ETM) after ETM, and also ETM for 6 days and then the coil spring was removed for a day (6d ETMR). These treatments were performed under isoflurane anesthesia (Fig. 1C).

Optical imaging/Mechanical stimulation of the incisor and molar/Data analysis

These methods were described in Chapter 1.

Statistics

The data are expressed as the mean ± SEM. SigmaStat software (ver. 4.0, Systat Software, San Jose, CA, USA) was used in comparison of the 4 ETM groups to the control. A probability value of $P < 0.05$ was considered statistically significant.

To depict any shape differences in the triangles, which were composed of the regions of the initial responses evoked by mechanical stimulation of the tooth, the thin-plate spline (tpsSplin Ver 1.22.; http://life.bio.sunysb.edu/morph/) was used as a deformation of one triangle into another using an algorithm that interpolates potential changes between landmarks of a reference shape and the shape of the ETM models. These shape differences could also be visualized using vectors of each landmark showing the magnitude and direction of the differences at each landmark. The thin-plate spline was also used to detect a set of shape variables, or partial warps that capture the shape differences among the objects being compared (Sibony et al., 2014).

Results

The sequential changes in the excitation of S1 and S2/IOR in response to mechanical stimulation of the incisors and first molar were elucidated (Fig. 1B) in the control and 1d ETM, 3d ETM, 7d ETM, and 6d ETMR (Fig. 1C).

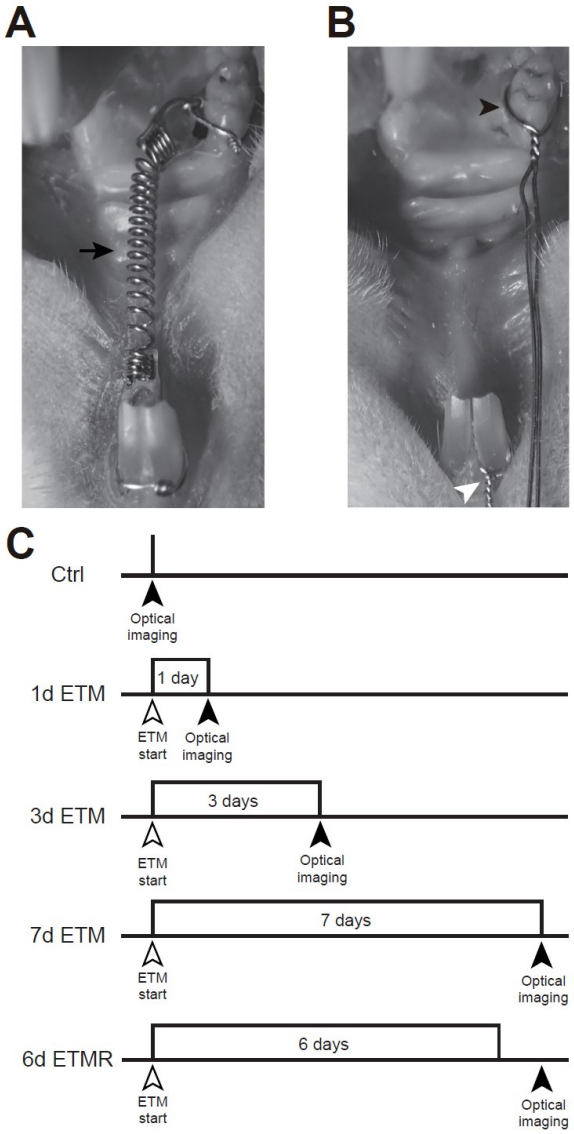

Figure 1. Schematic of ETM and methodology of mechanical stimulation. (A) Fixation of an orthodontic coil spring for ETM. Ligation between the maxillary incisors and right first molar using a nickel-titanium coil spring (arrow). (B) The coil spring was removed, and the ligature wires were ligated to the cervical area of the maxillary incisor (open arrowhead) and right maxillary first molar (closed arrowhead) before craniotomy. The photographs of (A) and (B) were taken without bonding using dental cement to show the fixation method clearly. (C) The scheme for the experimental schedule of ETM (open stripes with open arrowheads) and optical imaging (closed arrowheads).

Cortical excitation in response to maxillary incisor stimulation

As I previously reported, mechanical stimulation of the incisor in a control evoked an initial response in S2/IOR, the caudal region adjacent to MCA, and, almost simultaneously, separate excitation emerged in the rostroventral part of S1 (Fig. 2A,B; Kaneko et al., 2017). The excitation area expanded in a concentric manner (Fig. 2A). Because of the variation of the slack in the wire that transmits the mechanical stimulation from the motor unit to the teeth, I could not accurately estimate the latency of cortical excitation induced by mechanical stimulation.

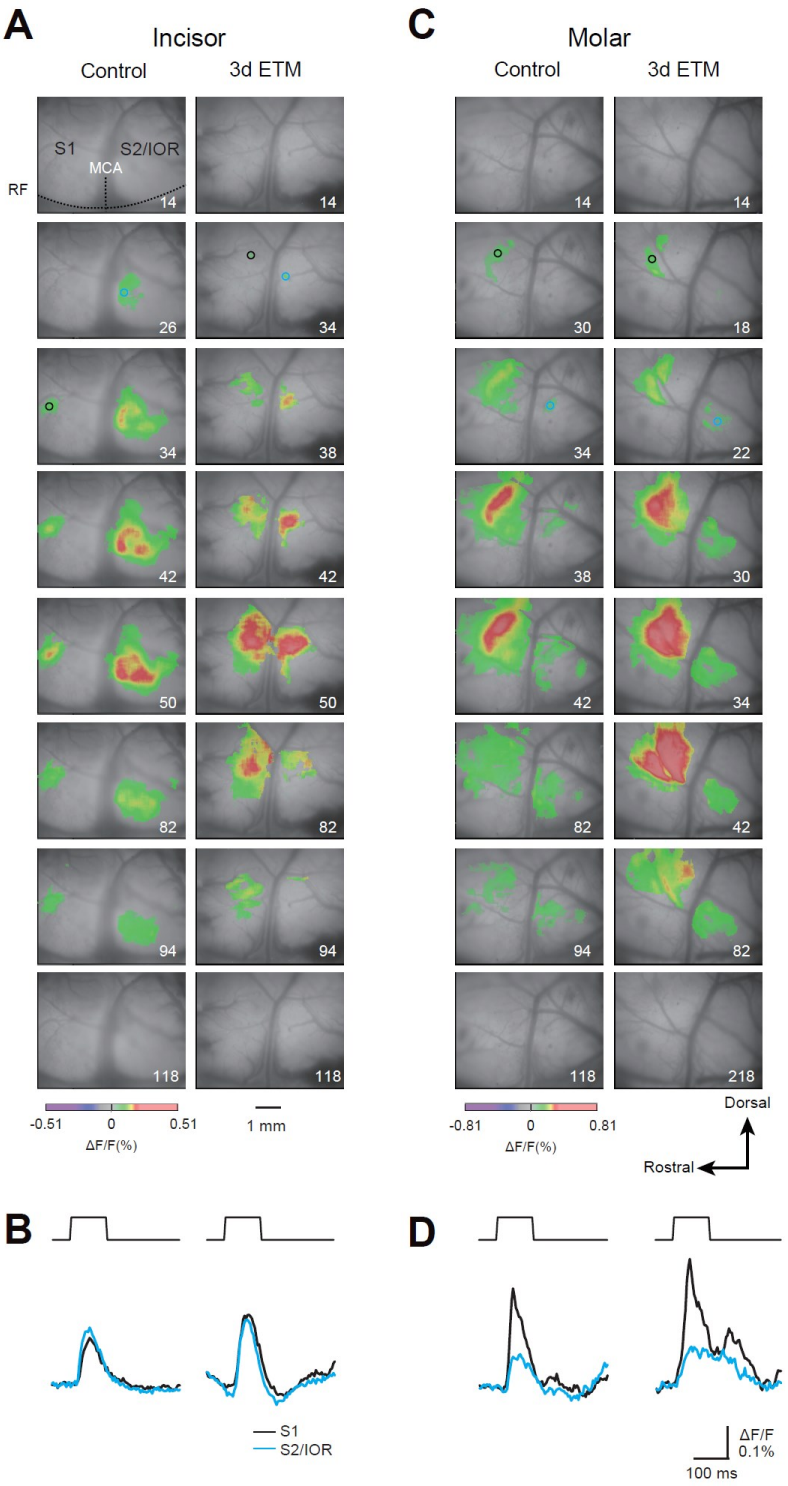

Figure 2. Spatiotemporal patterns of the responses to mechanical stimulation of the maxillary incisor or molar in a control and 3d ETM. (A) Excitatory propagation corresponding to mechanical stimulation of the incisor (duration = 100 ms) in the control (left column). The dotted lines delineate the MCA and RF. The second frame (26 ms) indicates the initial response that shows detectable excitation in S2/IOR (blue circle). In 3d ETM (right column), the initial response occurred in S1 (black circle) and S2/IOR (blue circle). The latency from the application of mechanical stimulation is shown in the bottom right corner (ms). (B) The temporal profiles of optical signals at the center of excitation in the control are marked with black (S1) and blue (S2/IOR) circles, as shown in (A). The square wave pulse indicates the voltage applied to the motor unit. (C) Excitatory propagation corresponding to mechanical stimulation of the first molar of the control (left column) and 3d ETM (right column). (D) The temporal profiles of optical signals at the center of excitation marked with black (S1) and blue (S2/IOR) circles in (C).

In a 3d ETM, an initial response in S1 to mechanical stimulation of the incisor was shifted toward the dorsocaudal region in comparison to that in the control, though the initially activated region in S2/IOR was located in a comparable region between the 3d ETM and the control (Fig. 2A). The peak amplitude of the initially responding regions of S1 and S2/IOR were tended to be larger than those of the control (Fig. 2A,B). The subsequent responses after the initial response in the 3d ETM showed a concentric expanding manner as in the control, and no separate excitation was observed in the rostroventral S1 region where the initial excitation was observed in the control (Fig. 2A).

Cortical excitation in response to maxillary molar stimulation

My previous study revealed the topographically organized representation of cortical responses to electrical and mechanical stimulation of the maxillary first molar (Kaneko et al., 2017). In agreement with that study, mechanical stimulation of the maxillary first molar induced an initial excitation both in S2/IOR caudally adjacent to the MCA and in the rostrodorsal S1 (Fig. 2C). This spatial pattern of excitation was maintained across the ETM models. A typical example of the excitation pattern of a 3d ETM demonstrated spatially similar initial responses in S2/IOR and S1 in the control (Fig. 2C). The peak amplitudes of the regions initially responded in S1 and S2/IOR were comparable to that of the control (Fig. 2C,D).

Quantification of spatiotemporal profiles of excitatory propagation

For the comparison of the topographic distribution pattern of the cortical responses to mechanical stimulation of the maxillary incisor or first molar in the control and ETM models, the maximum responses were superimposed in reference to the MCA and RF (Fig. 3A,B). The outlines of the excitatory regions commonly activated in 70% of the animals are depicted with bold lines.

In the responses to incisor stimulation, the total excitatory areas including responses in S1 and S2/IOR were not significantly different between the control and ETM models ($P = 0.22$, ANOVA; Fig. 3A,C). On the other hand, in terms of the excitation in response to molar stimulation, the total excitatory area in the 1d ETM was expanded (control, n = 11; 1d ETM, n = 12; $P = 0.005$, ANOVA with Dunnett's test), which recovered to the control level within 3 days (Fig. 3B,C).

The peak amplitude of the initially activated regions in S1 and S2/IOR that responded to incisor stimulation was comparable between the control and ETM models ($P > 0.08$, ANOVA on ranks; Fig. 3D). In contrast, molar stimulation induced an enhanced peak amplitude of excitation in S1 of 1d ETM (Fig. 3D); the excitation returned to the control level within 3 days. No significant change was observed in S2/IOR.

Changes in the topographic organization of excitatory propagation in S1

Although the maximum responses to incisor stimulation in S2/IOR were evoked in a similar region among the control (Fig. 3A, closed arrowhead) and ETM models, the maximum responses in S1 shifted toward the dorsocaudal region activated by molar stimulation in the control (Fig. 3B, open arrowhead). This shift in the excitatory region of S1 was observed not in the 1d ETM but in the 3d and 7d ETM. Only one day after removal of the coil spring, the shifted excitatory region in S1 returned to the control region (6d ETMR in Fig. 3A). On the

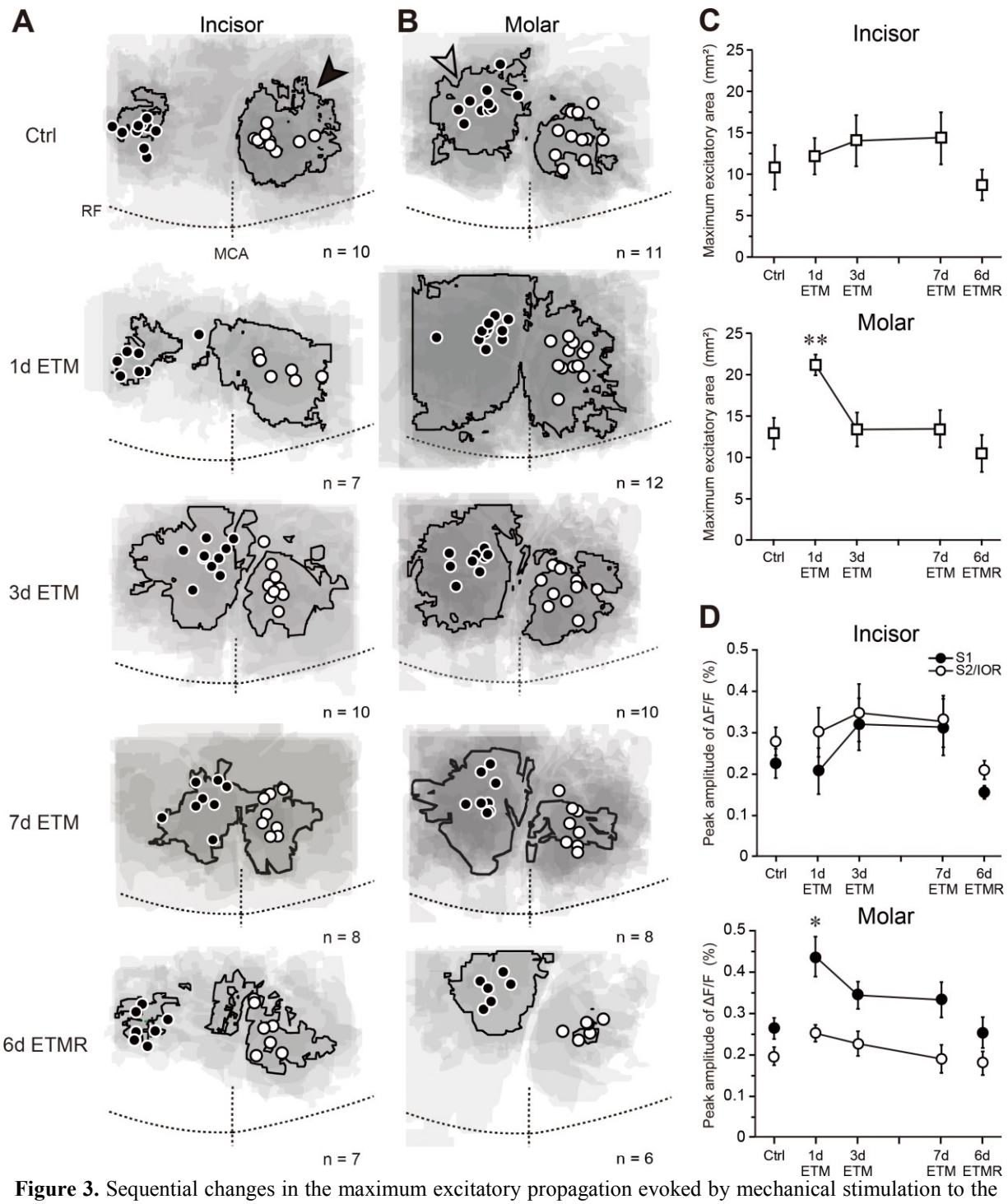

Figure 3. Sequential changes in the maximum excitatory propagation evoked by mechanical stimulation to the maxillary incisor and first molar in the control (Ctrl) and ETM models. (A, B) The maximum responses to incisor stimulation (A) and molar stimulation (B) are superimposed in reference to the MCA and RF (n = 6-12). Locations with maximum amplitude in S1 and S2/IOR are indicated by black and white circles, respectively. The denser colored area indicates a more commonly activated area among the rats. The bold lines indicate the overlapping area of the maximum responses in 70% of the rats. Closed and open arrowheads indicate the overlapped responses in S2/IOR, and S1, respectively. (C, D) The maximum excitatory area (C) and peak amplitude in S1 and S2/IOR (D) in each group. * $P < 0.05$, ANOVA on ranks with Dunn's test, ** $P < 0.01$, ANOVA with Dunnett's test, in which each ETM model is compared to the control

other hand, the excitation of S1 in response to molar stimulation was almost comparable to that of the control except for the expanded response in 1d ETM (Fig. 3B).

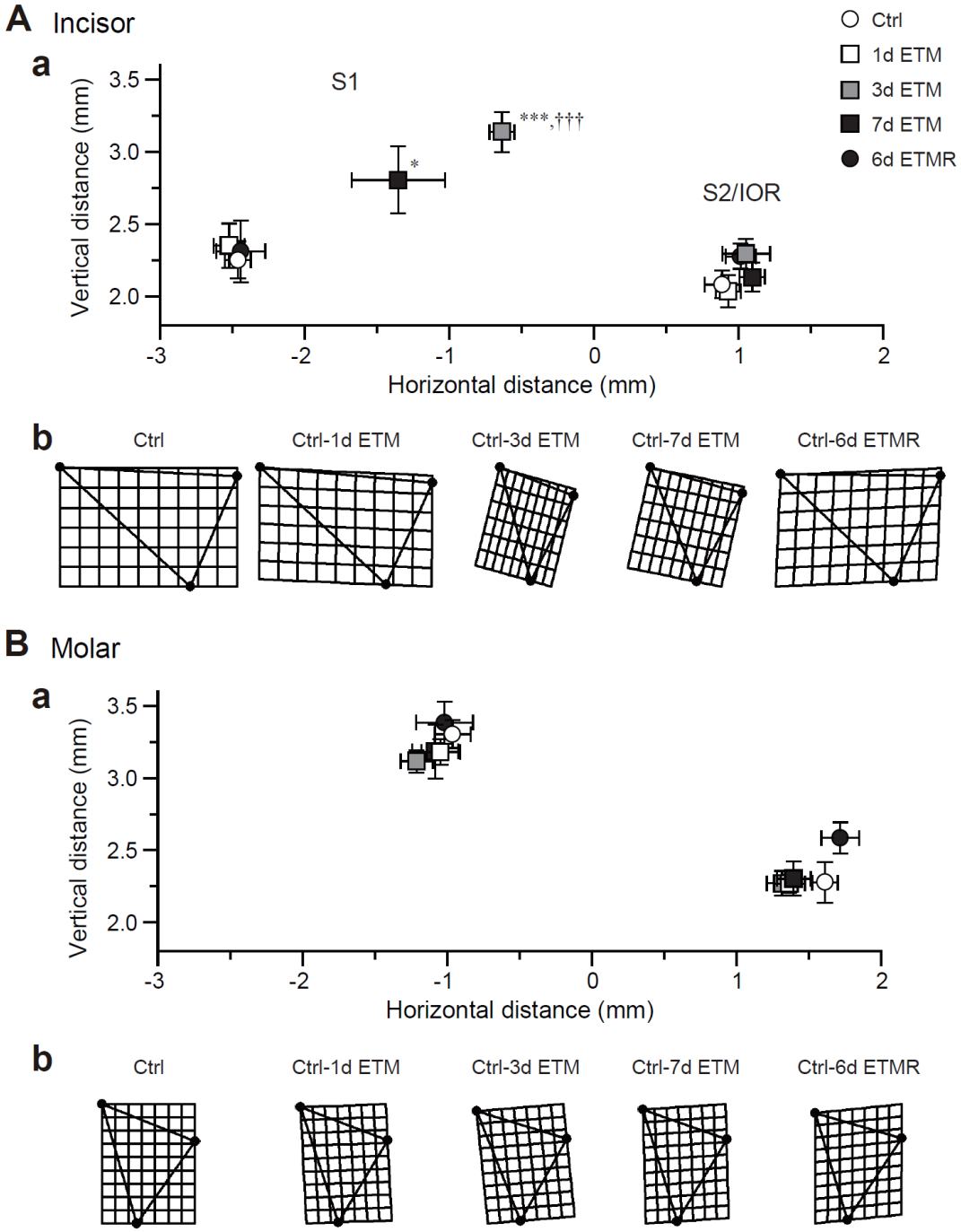

Figure 4. The coordinates of the center of the initially excited region responding to mechanical stimulation of the incisor (Aa) and molar (Ba) in the control and ETM models. The approximate line in reference to the RF was set as the horizontal axis, and the vertical axis was defined as the line that passed through the intersection of the MCA and RF and ran perpendicular to the horizontal axis. The intersection of the middle cerebral artery and RF was set as the origin. The center of gravity of the initial response evoked by mechanical stimulation of the maxillary incisor and first molar was plotted in the coordinates. * $P < 0.05$, *** $P < 0.001$, ANOVA on ranks with Dunn's test, in which the horizontal coordinate in each ETM group was compared to that in the control. ††† $P < 0.001$, ANOVA with Dunnett's test applied to the vertical coordinate. (Ab, Bb) To depict any shape differences in the triangles, which were the regions of the initial response in S1, S2/IOR, and the origin point, the thin-plate spline was used to deform the triangle into another using an algorithm that interpolates the potential changes between the landmarks of a reference shape and the shape in ETM models. Note the striking changes in the shape of 3d and 7d ETM in response to incisor stimulation.

To quantify the shift of the excitatory region in S1 and S2/IOR in ETM models, I obtained the approximate line representing RF and set it as the horizontal axis. The vertical axis was defined as the line that passed through the intersection of the MCA and RF and was defined as the origin, and perpendicular to the horizontal axis. The center of gravity of the initial response evoked by the mechanical stimuli to the maxillary incisor and first molar was plotted in the coordinates (Fig. 4).

In response to incisor stimulation, the horizontal distance of the excitatory regions in S1 from the vertical axis significantly decreased in 3d ETM (n = 10, $P < 0.001$, ANOVA on ranks with Dunn's test) and 7d ETM (n = 8, $P = 0.037$, ANOVA on ranks with Dunn's test) compared to the control (n = 10; Fig. 4Aa). In contrast, 1d ETM (n = 7) and 6d ETMR (n = 7) showed comparable values to those in the control. The vertical distance of the excitatory regions in S1 from the horizontal axis significantly increased in 3d ETM compared to the control ($P < 0.001$, ANOVA with Dunnett's test; Fig. 4Aa). In contrast, 1d and 7d ETM and 6d ETMR showed nonsignificant differences from that of the controls (1d ETM, $P = 0.985$; 7d ETM, $P = 0.081$; 6d ETMR, $P = 0.998$; ANOVA with Dunnett's test). In contrast to the distribution of the initial responses in S1, those in S2/IOR were comparable among the controls and ETM models ($P \geq 0.28$, ANOVA or ANOVA on ranks; Fig. 4Aa).

In contrast to incisor stimulation, all ETM models did not show significant changes in the coordinates either in S1 or S2/IOR responding to molar stimulation ($P \geq 0.08$, ANOVA; Fig. 4Ba).

To depict shape differences in the triangles composed by the origin and the center of gravity of the initial responses in S1 and S2/IOR, I used the thin-plate spline (see Experimental Procedure; Fig. 4Ab,Bb). This analysis demonstrated the differences in the shape of the triangle obtained from incisor stimulation in the control versus 3d and 7d ETM (Fig. 4Ab). In contrast, almost identical landmark shapes of the locations of the initial responses to molar stimulation were obtained from the control and ETM groups (Fig. 4Bb).

Discussion

The present optical imaging study demonstrated three major findings regarding cortical activities in ETM models. First, one day ETM induced expansion of excitatory propagation in response to mechanical stimulation of the maxillary molar principally in S1. Second, the center of excitation in S1 induced by incisor stimulation shifted toward the molar-responding region in ETM models. Third, the excitatory region in S2/IOR responding to the incisor and molar were located in the similar region during ETM. The spatial change in S1 is likely to be induced by simultaneous stimulation of the PDL, and might share the mechanisms of plastic changes in the barrel cortex induced by whisker pairing.

ETM-induced enhancement of excitatory propagation by molar stimulation

Previously, my colleagues have demonstrated that cortical excitation in S1 and S2/IOR in response to electrical stimulation of the PDL is facilitated by ETM (Horinuki et al., 2015, 2016). Mechanical stimulation applied in this study did not induce a jaw-opening reflex

(Kaneko et al., 2017), a possible parameter of noxious inputs (Mason et al., 1986). In addition, mechanical stimulation evoked less excitation in S2/IOR, which responds to noxious stimuli (Nakamura et al., 2015; Horinuki et al., 2015; Yokota et al., 2016a), compared to that induced by electrical stimulation (Kaneko et al., 2017). Therefore, not only nociception but also other somatosensations, including PDL sensation, are sensitive to and facilitated by ETM.

The facilitation of the cortical responses to molar mechanical stimulation by ETM was induced within a day. This finding is comparable to those of activity mapping studies demonstrating that ETM upregulates c-Fos expression and phosphorylation of ERK, both of which are neuronal activity markers in the nociception-related brain regions (Kato et al., 1994; Yamashiro et al., 1997; Fujiyoshi et al., 2000; Hiroshima et al., 2001; Magdalena et al., 2004; Joviliano et al., 2008; Hasegawa et al., 2012). The ETM-induced facilitative response of the peak amplitude of S1 in response to mechanical stimulation recovered to the control level within 3 days during ETM (Fig. 3D). This recovery time course is similar to that of my colleagues' previous finding that the facilitative response in S2/IOR to electrical stimulation of the PDL recovers to the control level within a week (Horinuki et al., 2016). The recovery time course of inflammation of the PDL correlates well with the facilitation of cortical excitatory propagation induced by electrical stimulation (Horinuki et al., 2016). Therefore, it is likely that PDL inflammation is a factor that is necessary for ETM-induced enhancement of nociception and mechanical sensation, which may be mediated by chemical mediators such as prostaglandins by lowering spike threshold of the peripheral sensory nerves (Krishnan et al., 2007).

ETM shifts the excitatory region in S1 but not in S2/IOR

ETM for 3 days induced a shift in the incisor-responding region to the molar-responding region in S1, though the incisor and the first molar were still greatly separated (Horinuki et al., 2016). Therefore, this shift is likely to be induced by changes in the neural circuits of the central nervous system. In ETM models, mechanical incisor stimulation activates PDL receptors both in the incisor itself and in the molar because of the connection between the incisor and the molar with the coil spring. These simultaneous mechanical inputs could induce synchronized ascending inputs in the secondary sensory neurons and the higher brain.

Synchronization of neural inputs is a critical factor that induces plastic changes in the neural circuits of the cerebral cortex. A typical example is whisker pairing, which changes neural responses in the barrel cortex; an increased response to both the principal and its paired neighbor whiskers (Diamond et al., 1993). This finding can be adapted to the present study, which involved pairing an incisor and molar with the coil spring, and may share similar mechanisms to induce the plastic change in S1. An additional finding of this study was that a plastic change was prominent in S1 rather than in S2/IOR.

Discrepancy in the effects of ETM between incisor and molar stimulation

Even though the incisor and molar were simultaneously stimulated during ETM, the reason

why the excitatory region in the molar did not shift to the incisor region in S1 is still unknown. In addition, it is curious that the enhancement of the peak amplitude of excitation in S1 was observed with molar stimulation but not with incisor stimulation. The anatomical structures of the dental root are different between the incisor and the molar. The root of the molar is similar to that of a human tooth; the apex of the root forms a narrow canal. In contrast, the rat incisor has a wide-opened canal in the apex that continues to erupt (Ohshima et al., 2005). The direction of the force exerted during mastication is also different between the incisor and molar. These differences might be reasons for the discrepancy in the plastic changes, however, this issue should be further examined.

The initial response to incisor stimulation in S1 of 3d and 7d ETM emerged in the molar-responsive region, and the center of excitation remained at the initially responding region. These results suggest that the shift is principally generated in thalamocortical or subcortical but not corticocortical connections. It is considered that the original pathway from the thalamus to the incisor region of S1 does not disappear because the activated region of the incisor rapidly returned to the level of the control one day after the coil removal.

Clinical implications

Pain and discomfort in patients tend to appear a day after the application of orthodontic forces, last for a few days, and disappear approximately 7 days after treatment (Ngan et al., 1989; Krishnan, 2007). This time course of clinical symptoms is different from that of this study. However, the easy recovery of the topographic changes in the excitatory regions in S1 may explain the clinical finding that abnormal sensation in the location of the teeth seldom occurs after orthodontic treatment. Experience-dependent cortical plasticity induced by sensory disturbance such as monocular deprivation has a critical period (Hensch, 2005). The present temporary shift of the incisor-responding region in S1 might be prolonged if ETM is applied in younger age. It is also interesting to examine whether similar change and recovery occur in older adult animals, which generally exhibit less plasticity than younger animals. Age-dependent plastic changes in S1 and S2/IOR by ETM should be next explored.

Conclusions

To elucidate how orthodontic treatment modulates somatosensory brain functions, I focused on the sequential changes in cortical excitation evoked by PDL mechanical stimulation during ETM. Electrical stimulation of the PDL induced jaw-opening reflex, in contrast, the mechanical stimulation of the molar did not induce the EMG activities, suggesting that the electrical stimulation but not the mechanical stimulation was noxious. The cortical response in S2/IOR evoked by the electrical stimulation of the PDL was more potently depressed compared to that in S1 by morphine. This finding demonstrates that S2/IOR but not S1 is involved in nociceptive information processing. In addition, ETM for 3 days induced a shift in the incisor-responding region to the molar-responding region in S1. Only one day after removal of the coil spring, the shifted excitatory region in S1 returned to the control region. This rapid recovery of the topographic shifts in the excitatory regions in S1 may explain the clinical finding that abnormal sensation in the location of the teeth seldom occurs after orthodontic treatment.

Acknowledgements

I am grateful to Prof. Motoyoshi for the opportunity to perform this study, Prof. Kobayashi for his instruction of this study, and colleagues in Department of Pharmacology for their technical advice and assistance.

References

Bereiter DA, Okamoto K. 2011. Neurobiology of estrogen status in deep craniofacial pain. Int Rev Neurobiol. 97, 251-284.

Burkey AR, Carstens E, Wenniger JJ, Tang J, Jasmin L. 1996. An opioidergic cortical antinociception triggering site in the agranular insular cortex of the rat that contributes to morphine antinociception. J Neurosci. 16, 6612-6623.

Byers MR. 1985. Sensory innervation of periodontal ligament of rat molars consists of unencapsulated Ruffini-like mechanoreceptors and free nerve endings. J Comp Neurol. 231, 500-518.

Dallel R, Luccarini P, Molat JL, Woda A. 1996. Effects of systemic morphine on the activity of convergent neurons of spinal trigeminal nucleus oralis in the rat. Eur J Pharmacol. 314, 19-25.

Diamond ME, Armstrong-James M, Ebner FF. 1993. Experience-dependent plasticity in adult rat barrel cortex. Proc Natl Acad Sci U S A. 90, 2082-2086.

Ettlin DA, Zhang H, Lutz K, Järmann T, Meier D, Gallo LM, Jäncke L, Palla S. 2004. Cortical activation resulting from painless vibrotactile dental stimulation measured by functional magnetic resonance imaging (fMRI). J Dent Res. 83, 757-761.

Fujita S, Kaneko M, Nakamura H, Kobayashi M. 2017. Spatiotemporal profiles of proprioception processed by the masseter muscle spindles in rat cerebral cortex: an optical imaging study. Front Neural Circuits. 11, 4.

Fujita S, Kitayama T, Mizoguchi N, Oi Y, Koshikawa N, Kobayashi M. 2012. Spatiotemporal profiles of transcallosal connections in rat insular cortex revealed by *in vivo* optical imaging. Neuroscience. 206, 201-211.

Fujiyoshi Y, Yamashiro T, Deguchi T, Sugimoto T, Takano-Yamamoto T. 2000. The difference in temporal distribution of c-Fos immunoreactive neurons between the medullary dorsal horn and the trigeminal subnucleus oralis in the rat following experimental tooth movement. Neurosci Lett. 283, 205-208.

Guo W, Wang H, Zou S, Wei F, Dubner R, Ren K. 2010. Long lasting pain hypersensitivity following ligation of the tendon of the masseter muscle in rats: a model of myogenic orofacial pain. Mol Pain. 15, 6-40.

Habre-Hallage P, Dricot L, Hermoye L, Reychler H, van Steenberghe D, Jacobs R, Grandin CB. 2014. Cortical activation resulting from the stimulation of periodontal mechanoreceptors measured by functional magnetic resonance imaging (fMRI). Clin Oral Invest. 18, 1949-1961.

Hannam AG. 1969. The response of periodontal mechanoreceptors in the dog to controlled loading of the teeth. Arch Oral Biol. 14, 781-791.

Hasegawa M, Kondo M, Suzuki I, Shimizu N, Sessle BJ, Iwata K. 2012. ERK is involved in tooth-pressure-induced Fos expression in Vc neurons. J Dent Res. 91, 1141-1146.

Hensch TK. 2005. Critical period plasticity in local cortical circuits. Nat Rev Neurosci. 6, 877-888.

Hiroshima K, Maeda T, Hanada K, Wakisaka S. 2001. Temporal and spatial distribution of Fos protein in the parabrachial nucleus neurons during experimental tooth movement of the rat molar. Brain Res. 908, 161-173.

Horinuki E, Shinoda M, Shimizu N, Koshikawa N, Kobayashi M. 2015. Orthodontic force facilitates cortical responses to periodontal stimulation. J Dent Res. 94, 1158-1166.

Horinuki E, Yamamoto K, Shimizu N, Koshikawa N, Kobayashi M. 2016. Sequential changes in cortical excitation during orthodontic treatment. J Dent Res. 95, 897-905.

Ishii N, Soma K, Toda K. 2002. Response properties of periodontal mechanoreceptors in rats. *in vitro*. Brain Res Bull. 58, 357-361.

Jiang C, Li Z, Quan H, Xiao L, Zhao J, Jiang C, Wang Y, Liu J, Gou Y, An S, Huang Y, Yu W, Zhang Y, He W, Yi Y, Chen Y, Wang J. 2015. Osteoimmunology in orthodontic tooth movement. Oral Dis. 21, 694–704.

Joviliano P, Junqueira AA, Stabile AC, Leite-Panissi CR, Rocha MJ. 2008. Rapid maxillary expansion causes neuronal activation in brain structures of rats. Brain Res Bull. 76, 396-401.

Kaneko M, Horinuki E, Shimizu N, Kobayashi M. 2017. Physiological profiles of cortical responses to mechanical stimulation of the tooth in the rat: An optical imaging study. Neuroscience. 358, 170-180.

Kato J, Wakisaka S, Tabata MJ, Sasaki Y, Kurisu K. 1994. Induction of Fos protein in the rat trigeminal nucleus complex during an experimental tooth movement. Arch Oral Biol. 39, 723-726.

Kato T, Kawamura Y, Morimoto T. 1982. Branching of muscle spindle afferents of jaw closing muscles in the cat. J Physiol. 323, 483-495.

Kieffer BL, Gaveriaux-Ruff C. 2002. Exploring the opioid system by gene knockout. Prog Neurobiol. 66, 285-306.

Kobayashi M, Horinuki E. 2017. Neural mechanisms of nociception by orthodontic treatment. J Oral Sci. 59, 167-171.

Krishnan V, Davidovitch Z. 2006. Cellular, molecular, and tissue-level reactions to orthodontic force. Am J Orthod Dentofacial Orthop. 129, 469.e1-32.

Krishnan V. 2007. Orthodontic pain: from causes to management--a review. Eur J Orthod. 29, 170-179.

Kuki F, Sugiyo S, Abe T, Niwa H, Takemura M. 2014. Inferior alveolar nerve transection enhanced formalin-induced nocifensive responses in the upper lip: systemic buprenorphine had more antinociceptive efficacy over morphine. Pharmacology. 93, 10-17.

Lee SY, Yoo HI, Kim SH. 2015. CCR5-CCL axis in PDL during orthodontic biophysical force application. J Dent Res. 94, 1715-1723.

Lin LD, Murray GM, Sessle BJ. 1994. Functional properties of single neurons in the primate face primary somatosensory cortex. I. Relations with trained orofacial motor behaviors. J Neurophysiol. 71, 2377-2390.

Linden RW. 1990. An update on the innervation of the periodontal ligament. Eur J Orthod. 12, 91-100.

Luccarini P, Childeric A, Gaydier AM, Voisin D, Dallel R. 2006. The orofacial formalin test in the mouse: a behavioral model for studying physiology and modulation of trigeminal nociception. J Pain. 7, 908-914.

Lund JP, Sessle BJ. 1974. Oral-facial and jaw muscle afferent projections to neurons in cat frontal cortex. Exp Neurol. 45, 314-331.

Lund JP, Kolta A. 2006. Generation of the central masticatory pattern and its modification by sensory feedback. Dysphagia. 21, 167-174.

Magdalena CM, Navarro VP, Park DM, Stuani MB, Rocha MJ. 2004. c-fos expression in rat brain nuclei following incisor tooth movement. J Dent Res. 83, 50-54.

Mason P, Strassman A, Maciewicz R. 1985. Is the jaw-opening reflex a valid model of pain? Brain Res. 357, 137-146.

Mason P, Strassman A, Maciewicz R. 1986. Intracellular responses of raphe magnus neurons during the jaw-opening reflex evoked by tooth pulp stimulation. Brain Res. 379, 232-241.

McDonald J, Lambert DG. 2005. Opioid receptors. CEACCP. 5, 22-25.

McDonald J, Lambert DG. 2013. Opioid mechanisms and opioid drugs. Anaesth Intensive Care Med. 14, 505-509.

Morimoto T, Inoue T, Masuda Y, Nagashima T. 1989. Sensory components facilitating jaw-closing muscle activities in the rabbit. Exp Brain Res. 76, 424-440.

Nakamura H, Kato R, Shirakawa T, Koshikawa N, Kobayashi M. 2015. Spatiotemporal profiles of dental pulp nociception in rat cerebral cortex: An optical imaging study. J Comp Neurol. 523, 1162-1174.

Nakamura H, Shirakawa T, Koshikawa N, Kobayashi M. 2016. Distinct excitation to pulpal stimuli between somatosensory and insular cortices. J Dent Res. 95, 180-187.

Ness AR. 1954. The mechanoreceptors of the rabbit mandibular incisor. J Physiol. 126, 475-493.

Ngan P, Kess B, Wilson S. 1989. Perception of discomfort by patients undergoing orthodontic treatment. Am J Orthod Dentofacial Orthop. 96, 47-53.

Nishiura H, Tabata T, Watanabe M. 2000. Response properties of slowly and rapidly adapting periodontal mechanosensitive neurones in the primary somatosensory cortex of the cat. Arch Oral Biol. 45, 833-842.

Ogawa H, Ito S, Nomura T. 1989. Oral cavity representation at the frontal operculum of macaque monkeys. Neurosci Res. 6, 283-298.

Ohshima H, Nakasone N, Hashimoto E, Sakai H, Nakakura-Ohshima K, Harada H. 2005. The eternal tooth germ is formed at the apical end of continuously growing teeth. Arch Oral Biol. 50, 153-157.

Shigenaga Y, Matano S, Kusuyama M, Sakai A. 1974. Cortical neurons responding to electrical stimulations of the rat's incisor pulp. Brain Res. 67, 153-156.

Sibony P, Strachovsky M, Honkanen R, Kupersmith MJ. 2014. Optical coherence tomography shape analysis of the peripapillary retinal pigment epithelium layer in presumed optic nerve sheath meningiomas. J Neuroophthalmol. 34, 130-136.

Sood M, Bhatt P, Sessle BJ. 2015. Mechanical and thermal hypersensitivities associated with orthodontic tooth movement: a behavioral rat model for orthodontic tooth movement-induced pain. J Oral Facial Pain Headache. 29, 60-69.

Tadokoro O, Maeda T, Heyeraas KJ, Vandevska-Radunovic V, Kozawa Y, Hals Kvinnsland I. 2002. Merkel-like cells in Malassez epithelium in the periodontal ligament of cats: an immunohistochemical, confocal-laser scanning and immuno electron-microscopic investigation. J Periodontal Res. 37, 456-463.

Taira K. 1987. Characteristics of periodontal mechanosensitive neurons in the first somatosensory cortex of the cat. Brain Res. 409, 52-61.

Toda T, Taoka M. 2001. The complexity of receptive fields of periodontal mechanoreceptive neurons in the postcentral area 2 of conscious macaque monkey brains. Arch Oral Biol. 46, 1079-1084.

Tzabazis A, Klyukinov M, Manering N, Nemenov MI, Shafer SL, Yeomans DC. 2005. Differential activation of trigeminal C or Adelta nociceptors by infrared diode laser in rats: behavioral evidence. Brain Res. 1037, 148-156.

Vandevska-Radunovic V. 1999. Neural modulation of inflammatory reactions in dental tissues incident to orthodontic tooth movement. A review of the literature. Eur J Orthod. 21, 231-247.

Watanabe M, Tabata T, Karita K. 1991. Facilitatory effect of jaw opening on somatosensory (SI) cortical neurones sensitive to tooth pressure in the cat. Arch Oral Biol. 36, 899-903.

Woda A, Pionchon P. 2000. A unified concept of idiopathic orofacial pain: pathophysiologic features. J Orofac Pain. 14, 196-212.

Wong-Riley. 1979. Changes in the visual system of monocularly sutured or enucleated cats demonstrable with cytochrome oxidase histochemistry. Brain Res. 171, 11-28.

Yamashiro T, Nakagawa K, Satoh K, Moriyama H, Takada K. 1997. c-fos expression in the trigeminal sensory complex and pontine parabrachial areas following experimental tooth movement. Neuroreport. 8, 2351-2353.

Yeomans DC, Cooper BY, Vierck CJ Jr. 1995. Comparisons of dose-dependent effects of systemic morphine on flexion reflex components and operant avoidance responses of awake non-human primates. Brain Res. 670, 297-302.

Yokota E, Koyanagi Y, Nakamura H, Horinuki E, Oi Y, Kobayashi M. 2016a. Opposite effects of mu and delta opioid receptor agonists on excitatory propagation induced in rat somatosensory and insular cortices by dental pulp stimulation. Neurosci Lett. 628, 52-58.

Yokota E, Koyanagi Y, Yamamoto K, Oi Y, Koshikawa N, Kobayashi M. 2016b. Opioid subtype- and cell-type-dependent regulation of inhibitory synaptic transmission in the rat insular cortex. Neuroscience. 339, 478-490.

Zhang W, Kobayashi M, Moritani M, Masuda Y, Dong J, Yagi T, Maeda T, Morimoto T. 2003. An involvement of trigeminal mesencephalic neurons in regulation of occlusal vertical dimension in the guinea pig. J Dent Res. 82, 565-569.

Zollner C, Stein C. 2007. Opioids. In: Analgesia. Handb Exp Pharmacol. vol. 177 (Christoph Stein ed), Springer, Berlin, 31-63.